

A Software Tool for Automatic Geometry Generation of a Micro Turbine

Simon P. HOFFMANN
Frank U. RÜCKERT
Danjana THEIS
Alexander G. RUFFINO
Daniel LEHSER-PFEFFERMANN
Dirk HÜBNER

*University of Applied Sciences Saarbrücken
Saarbrücken, Germany
frank.rueckert@htwsaar.de*

Received (26 June 2018)

Revised (27 August 2018)

Accepted (30 August 2018)

Heat recovery plays an important role in increasing the efficiency of renewable energy facilities like biomass furnaces, solar power plants or biofuel combustion engines. As the overall efficiency of the facilities can be increased by recovering the energy. The available waste heat can be converted directly into mechanical energy, pressure or subsequently converted into electrical energy by coupling the expansions machine with a generator. The waste heat can be converted by Organic Rankine Cycle (ORC). Therefore, an expansion machine, e.g. a turbine is required. Also small amounts of waste heat can be recovered, if so-called micro turbines are used. Design and construction of such micro turbines always follow fixed rules. Aim of this work is to explain the rules how to design a micro turbine. Furthermore, our workflow and a software tool which follows these rules should be presented.

Keywords: organic Rankine cycle (ORC), micro turbine, computational fluid dynamics (CFD), fused deposition modeling (FDM), waste heat recovery (WHR).

1. Introduction

To investigate the heat recovery potential through the use of exhaust gas at rolling mill furnaces, University of Applied Sciences Saarbrücken (htw saar) has already carried out by Paulus [1]. Based on the previous study, the concrete geometry of a vapor turbine is now to be developed [2-4]. Each turbine needs a special design according to its parameters like mass throughput, pressures, etc. as described by Ringler, et al. [5, 6].

Today, this design for optimized turbines is usually carried out by Computational Fluid Dynamics (CFD) and delivers optimized flow cross-sections in the turbine [7]. In addition, the inflow and outflow (volute) must of course be geometrically optimized. Based on these individual simulation data, the geometry for the turbine wheel and the stator and thus the maximum mechanical power that can be generated is determined. This in turn determines the speed and torque, as well as the dimensions of the other components. Ultimately, this results in an individual size for each machine, which is reflected in the shaft diameter and the bearing size (rolling and slide bearings), where new calculations would have to be made for each modification of the turbine. In order to optimize this design process, an automated parameter-controlled generation of the necessary machine data is expedient.

The aim of this work is therefore to realize an automated parameter-controlled design of a turbine including the main components volute, turbine wheel, turbine housing, shaft and shaft bearing based on CFD data. The specification is that the design environment CATIA V5 R21 is used for this. The CFD data required for design are generated by the finite element program ANSYS CFX 18 [8], which is specially optimized for the calculation of fluid engineering problems. After CFD has determined the optimum geometry for the turbine wheel and the matching nozzle, these geometric data are to be imported into CATIA for the construction of the components [9].

2. Design concept

First step in the design process of a turbine must be the thermodynamic behavior of the process media. In general it can be said, the model and the full geometry must be built around the chemical or thermodynamic process. For a process media propane is used because of its major advantages as described in detail in this section.

2.1. Fluid properties and thermodynamics

Propane is easy to handle, available and not poisoning. The boiling temperature is rather low to fulfill our demands. In the $\log(p)$, h -diagram (see Fig. 1). The expansion process inside the turbine is shown. Further it can be seen, that propane has a dry expanding behavior, which helps to prevent droplet building inside the turbine. Droplets with high velocities can lead to erosion. The fluid properties of propane were taken from the tool LMS Imagine.Lab AMESim 15 [10].

Starting from thermodynamics, further design decisions are based on geometry of the volute of a standard turbocharger from automotive industry. Which can be seen in Fig. 2. Additionally a new rotor and stator has to be designed. However, a standard turbocharger from automotive industry differs significantly from energetic micro turbines. Outside the turbine, it consists of a compressor wheel. This is not included in ORC and was removed. Also bearing systems would be different, because of different working media. The turbocharger works with exhaust gas and the micro turbine works with propane, so material requirements will be different. In this preliminary work, not all of these requirements could be fulfilled, yet.

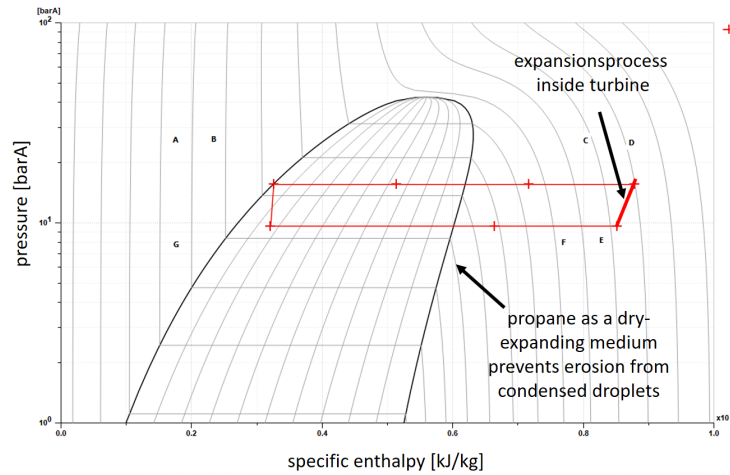


Figure 1 Thermodynamic behavior of the process media *propane* in characterized by the $\log(p)$, h -diagram [10]

2.2. Axial turbine type concept

The turbine to be developed is a 1-stage axial turbine, through which a fluid flows parallel to the turbine shaft. Accordingly, only one turbine wheel with upstream nozzle is required, which simplifies the design considerably. Although multi-stage turbines can in principle achieve higher efficiency, they also require comprehensive CFD analyses due to the increased complexity and the interactions between the individual turbine stages. The process medium (*here: propane*) is discharged via the volute in the direction indicated by the arrow.

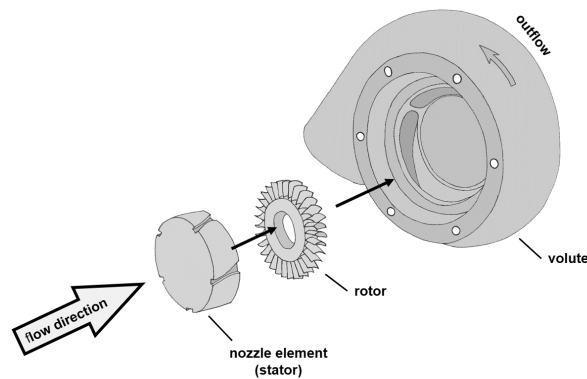


Figure 2 Overview over the design concept for an axial micro turbine for Organic Rankine Cycle

As shown in Fig. 2, the turbine consists of a nozzle body (stator), turbine wheel (rotor), shaft (not shown in the figure) and volute. The nozzle is to be designed as

a Laval nozzle, whereby several of these nozzle profiles are to be worked into the nozzle body all round.

The nozzle body is to be pressed into the inlet side of the turbine housing, i.e. it is flush with the inner wall so that the fluid used must definitely flow through the nozzles. In the nozzles, the pressure in the fluid is reduced and almost completely converted into kinetic energy by increasing the flow velocity (conservation of energy). Consequently, the narrowest cross-section of the nozzle is decisive for the mass flow and the resulting flow velocity. After passing the nozzle, the "fast fluid" hits the turbine wheel and sets it in motion. In the turbine wheel (rotor), this kinetic energy together with the thermal energy is then converted into mechanical work. This now drives the wave. If the shaft of the turbine wheel is connected to a suitable electrical machine (generator), the kinetic energy of the turbine wheel can be converted into electrical energy.

For further investigations computational fluid dynamics (CFD) simulations of the nozzle region (the Laval nozzle) and the rotor regions have to be done. For this, only one segment of the stator and one segment of the rotor are calculated because of high computational effort for the numerical simulations. The segments can be seen in Fig. 3. The full turbine consists of 3 segments for the Laval nozzle and 12 segments for the rotor.

2.3. Numerical results and analysis

The Computational Fluid Dynamics (CFD) analysis is based on the general-purpose code CFD ANSYS CFX 18 [8], applying the Finite Volume Method (FVM) for discretizing the governing differential equations. Given the scarcely used method of simulation with solving the Navier-Stokes equations, these settings and boundary conditions are essentially needed for comparison. Looking at the former listed works, Noll [11], Perić [7] and Menter [12] described those details of the mathematical and numerical formulation adequately. Fluid properties of propane have been taken from the ANSYS CFX data base.

In CFD, the transport equations are established, discretized and solved in numerical flow simulation. A closer look at all equations reveals that their structure is very similar. Therefore, it was possible to generalize these transport equations as follows [13, 14]:

$$\frac{\partial(\rho\Phi)}{\partial t} + \frac{\partial(\rho\nu_j\Phi)}{\partial x_j} = \frac{\partial}{\partial x_j} \left(\Gamma \frac{\partial(\Phi)}{\partial x_j} \right) + S_\Phi \quad (1)$$

The dependent variable Φ is replaced by the flow size that is currently of interest. Here Γ is the diffusion coefficient. If any transport equation is to be adapted to the general form, all terms that do not belong to convection or diffusion are gathered in the source term [11, 12]. The convective terms are discretized by a formally third-order accurate QUICK discretization scheme [15] for the Navier-Stokes equations and a second-order upwind discretization scheme (UDS) [15]. After the transport equations have been established, they are discretized to solve the fluid mechanics problem numerically. The total volume of the fluid is divided into small, discrete volumes. These are also called control volumes or cells [11, 16].

Turbulence is modelled by a two-equation turbulence model, that is, by the Shear Stress Transport (SST) model [12], which were shown to perform quite reliably

especially for wall-driven turbulent flows with potential to predict transitional effects [17, 15]. In this work, the turbulent kinetic energy k and the inverse time ω are used to describe the turbulent linear dimension L . The conservation equation for kinetic energy is modified as follows [12]:

$$\frac{\partial(\rho k)}{\partial t} + \frac{\partial(\rho \bar{u}_j k)}{\partial x_j} = P_k - \rho \beta^* k \omega + \frac{\partial}{\partial x_j} \left[\left(\mu + \frac{\mu_t}{\sigma_\omega^*} \right) \frac{\partial \omega}{\partial x_j} \right] \quad (2)$$

For the inverse time measure ω the following conservation equation can be used:

$$\frac{\partial(\rho \omega)}{\partial t} + \frac{\partial(\rho \bar{u}_j \omega)}{\partial x_j} = \alpha \frac{\omega}{k} P_k - \rho \beta \omega^2 + \frac{\partial}{\partial x_j} \left[\left(\mu + \frac{\mu_t}{\sigma_\omega^*} \right) \frac{\partial \omega}{\partial x_j} \right] \quad (3)$$

This results in the following correlation between linear measure L , vortex frequency ω and the turbulent kinetic energy k [18].

$$\omega = \frac{\sqrt{k}}{C_\mu L} \quad (4)$$

The k - ω model achieves very good and reliable results especially near the wall, while in the far field it shows worse results [11, 19]. The eddy viscosity is defined as:

$$\mu_t = \rho \frac{k}{\omega} \quad (5)$$

Flow turbulence is modelled within a RANS (Reynolds Averaged Numerical Simulation) approach [19], where the time-averaged equations are solved for the time-averaged variables in steady state.

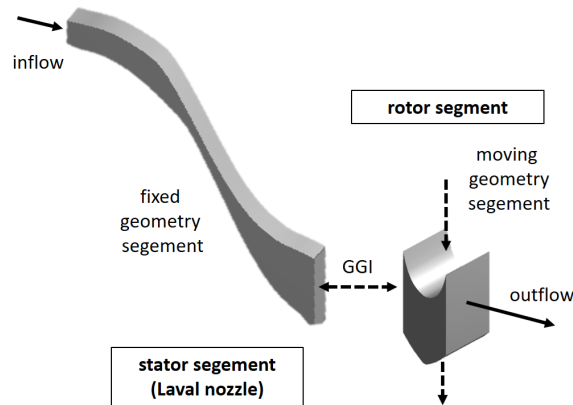


Figure 3 Geometry segments of one Laval nozzle (stator) and one rotor segment designed in ANSYS Design Modeler for examination of mass flow calculation and fluid flow behavior

The number of rotations as well as the power transfer to the shaft is defined by the rotor segment gap and the fluid flow behavior in this region. Turbulences and swirl can lower the efficiency of the turbine.

Both segments are clued together with a General Grid Interface (GGI). The flow has to be three-dimensional (3D) and statistically in the steady state. For a rotating turbine with fixed blades, this setting resembles a blade-to-blade surface at a fixed radial section, where the turbine rotational speed and the wind speed are constant in time, in a moving (i.e., rotating) reference frame. In the sense of a quasi-three dimensional procedure, which is also quite common in vapor and gas turbines [12]. A frozen rotor model was used. Here $r = 1000$ rev/s and an outlet pressure of 10 bar is assumed. For the segment regions a hex dominate mesh was produced with an approximately segment size of 0,0003 m and a node number of 61.426 control volumes.

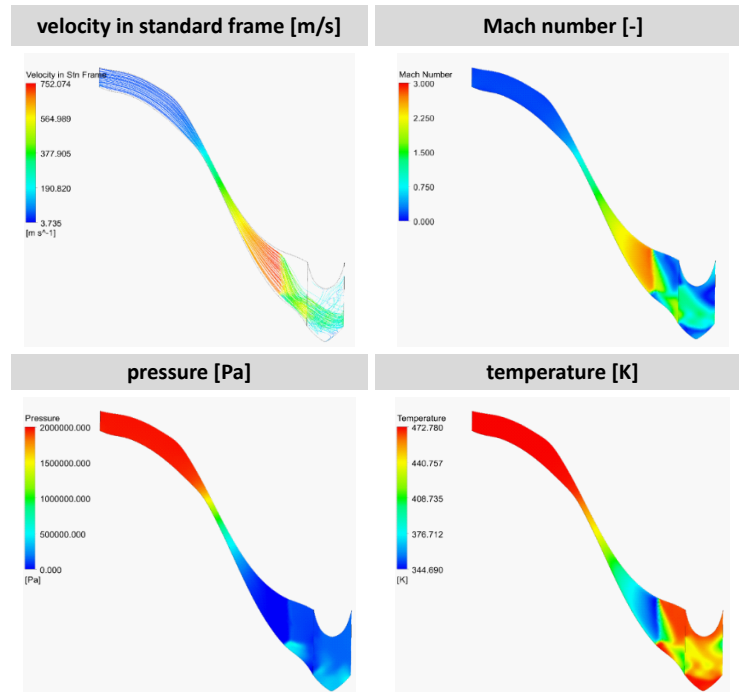


Figure 4 Numerical results from CFD inside Laval nozzle and rotor segment; streamlines in velocity standard frame, Mach number, pressure profiles, temperature distributions

Different load points have been examined, in Fig. 4 simulations with inlet pressure of 20 bar and outlet pressure of 10 bar are presented, which fits to the $\log(p)$, h -diagram shown in Fig. 1. The dilemma is, that optimization for one load point leads not necessarily to the optimum geometry of another load point. Which is a problem that can never be solved.

The presented design concept is based on the idea, that the full pressure and thermal energy inside the fluid will be converted into kinetic energy inside the Laval nozzle. Therefore, the mass flow inside the full turbine is defined by the narrowest gap in the turbine where Mach number $Ma = 1$ should be reached. All simulations in Fig. 4 where done with the fluid properties for propane implemented in CFX [8]. The simulations presented in Fig.4 are done with an inlet pressure of 20 bar before the nozzle and a mass flow of 0.004 kg/s. The temperature at the inlet of the nozzle region was 473 K. The results presented in Fig. 4 show a good pressure conversion to kinetic energy and a Mach number of 1 in the narrowest gap of the Laval nozzle.

3. Automatic geometry generation

The geometric data of the turbine wheel originate from the CFD simulation and are matched to the nozzle geometry used. In ANSYS, only the fluid space was calculated, which was then imported into CATIA [9] and removed from the cylindrical base body of the turbine wheel. In total, the turbine wheel was equipped with 12 blades.

3.1. Preprocessing with Microsoft Excel

To ensure that the preprocessing tool for Microsoft Excel does not produce incorrect results, it is important to adhere to a certain sequence during processing. For the sake of clarity, the Excel worksheet is divided into different tabs that could worked through from front to back.

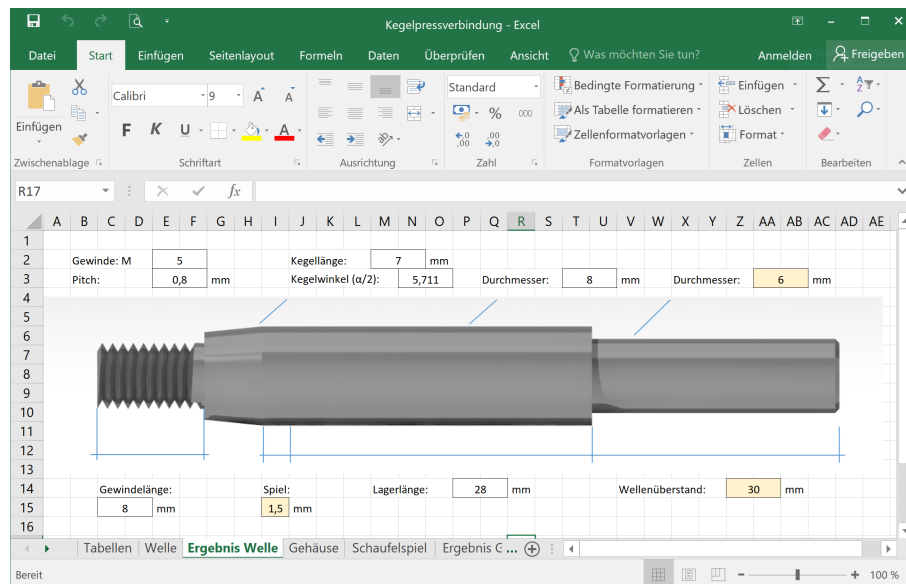


Figure 5 Microsoft Excel design tool with spread sheet for shaft design of the micro turbine

This results in the following sequence. Calculation of the shaft (step 1), calculation of the housing (step 2), calculation of the blade clearance (step 3), calculation of the mounting (step 4).

Since different calculation steps are based on each other from different networked tabs, failure to observe the specified sequence could lead to incorrect dimensioning. However, before the design of the various components can be started with the help of this Excel tool, the necessary preliminary considerations should be completed. These preliminary considerations include determining the nozzle and blade geometry (dimensions), which can be done in ANSYS, for example, as well as knowing the pressures in front of and behind the nozzle during operation, the temperature of the working medium, the speed of the turbine and the nominal torque. All this data is indispensable as input parameters for the Excel tool.

3.2. Determination of the shaft diameter

The following calculations are done according to [20]. Before the design, dimensioning of the shaft can be started, a number of parameters must be known. These include in particular the material properties of the material to be used and the torque T to be expected during operation. The CFD simulation showed that the nominal torque T_{nom} at operating speed ($n = 60,000rpm$) is set to 1 Nm. In combination with a safety factor $S = 1.3$, the torque T to be used for dimensioning the shaft can be determined.

$$T = T_{nenn} \cdot S = 1 \text{ Nm} \cdot 1.3 = 1.3 \text{ Nm}$$

Taking into account the application factor K_A (from TB 3-5) [20], which was set at 1.25 due to the shocks to be expected only moderately in later operation, the maximum power of the turbine:

$$P \approx \frac{T \cdot n}{9550 \cdot K_A} = \frac{1.3 \text{ Nm} \cdot 60000 \text{ min}^{-1}}{9550 \cdot 1.25} = 6.53 \text{ kW} \quad (6)$$

Finally, by knowing these data, the design diameter d' can be determined. To simplify matters, it is assumed that there is no bending moment, especially since the distance to the bearing is also relatively small.

$$d' \approx 570 \sqrt[3]{\frac{K_A \cdot P}{n \cdot \tau_{tSch}}} = 570 \sqrt[3]{\frac{1.25 \cdot 6.53 \text{ kW} \cdot \text{mm}^2}{60000 \text{ min}^{-1} \cdot 250 \text{ N}}} = 4.65 \text{ mm} \quad (7)$$

Since a shaft with diameter of 4.65 mm is quite fligree and thus problematic stresses would arise during the design of the subsequent interference fit, the selected diameter is set to 8 mm. As can also be seen from the above formula, it is assumed that the torsion is regarded as swelling. Actually, torsion will not swing periodically around mean torsional moment, but will be nearly constant, however minimum fluctuations can occur. Accordingly, a higher maximum permissible voltage could be expected. By using the torsional threshold strength, which is lower in terms of amount, the shaft is dimensioned a little thicker, which is equivalent to increased safety and has a positive effect on the overall service life of the shaft.

3.3. Dynamic strength analysis

To perform the dynamic strength analysis, the geometric factor K_g must first be determined. This factor depends both on the diameter of the shaft and on the type of loading.

$$K_g \approx 1 - 0.2 \frac{\log(d/7.5 \text{ mm})}{\log(20)} = 1 - 0.2 \frac{\log(8 \text{ mm}/7.5 \text{ mm})}{\log(20)} \approx 0.996 \quad (8)$$

In addition, the influencing factor of surface roughness $K_{0\sigma}$ for torsional stress is determined, which provides information on how the roughness (roughness depth Rz) of the shaft affects its fatigue strength.

$$K_{0\sigma} \approx 1 - 0.2 \log\left(\frac{Rz}{\mu\text{m}}\right) \left(\log\left(\frac{R_m}{20 \frac{\text{N}}{\text{mm}^2}}\right) - 1\right) \approx 1.27 \quad (9)$$

In this example calculation, $K_V = 1.2$ is assumed. With these data, it is now possible to determine the design factor for fatigue strength under torsional stress.

$$K_{Dt} = \left(\frac{\beta_{kt}}{K_g} + \frac{1}{K_{0\sigma}} - 1\right) \frac{1}{K_V} = \left(\frac{1}{0.996} + \frac{1}{1} - 1\right) \frac{1}{1.2} \approx 0.837 \quad (10)$$

The influencing factor can be used to calculate the maximum permissible design fatigue strength of the shaft material for dynamic strength. Of course, this value must not be exceeded by the torsional stress actually occurring during operation:

$$\tau_{tGW} = \frac{\tau_{tSch} \cdot K_t}{K_{Dt}} = \frac{250 \text{ N} \cdot 1}{\text{mm}^2 \cdot 0.837} \approx 298.7 \frac{\text{N}}{\text{mm}^2} \quad (11)$$

This results in the following safety against fatigue fracture:

$$S_D = \frac{\tau_{tGW}}{\tau_{ta}} = \frac{298.7 \text{ N} \cdot \text{mm}^2}{8.09 \text{ N} \cdot \text{mm}^2} \approx 37 \quad (12)$$

Since $S_D = 37$ is significantly higher than the minimum safety $S_{Dmin} = 1.5$ (compare TB 3-14a), it can be assumed that the shaft is also sufficiently strong for continuous operation [21].

The operation of this tool is largely self-explanatory. On the individual tabs of the worksheet, the materials of the components to be dimensioned are defined directly at the beginning. This is done in such a way that the desired material is referenced by a reference number. For this purpose, the "Tables" tab lists a collection of different materials including the corresponding reference number. If the reference number of the desired material has been entered, the table below is updated and indicates the corresponding material properties so that the user should be directly aware of any errors that may have occurred.

When designing micro turbines, the diameter of the shaft does not depend only on the strength conditions we used here. Diameter of bearings and generator also play a key role. The dynamics of the rotor should also be checked, e.g. critical speed and modal analysis by the tool ADAMS. This examination was not included here, and should be added in future to our workflow.

3.4. Interface from Microsoft Excel to CATIA V5

The results sheets provide a quick overview of all relevant design parameters. Altogether, there is one results sheet for each of the three main components of the turbine (shaft, turbine housing, bearing cover). The dimensions of the nozzle body and turbine wheel have already been known from ANSYS. The optically appealing preparation of this data, which is also identical to the graphical user interface of the CATIA macro, is intended to promote understanding and achieve the best possible user experience. Once all result sheets are available (for example as printout), you can switch to the CATIA macro.

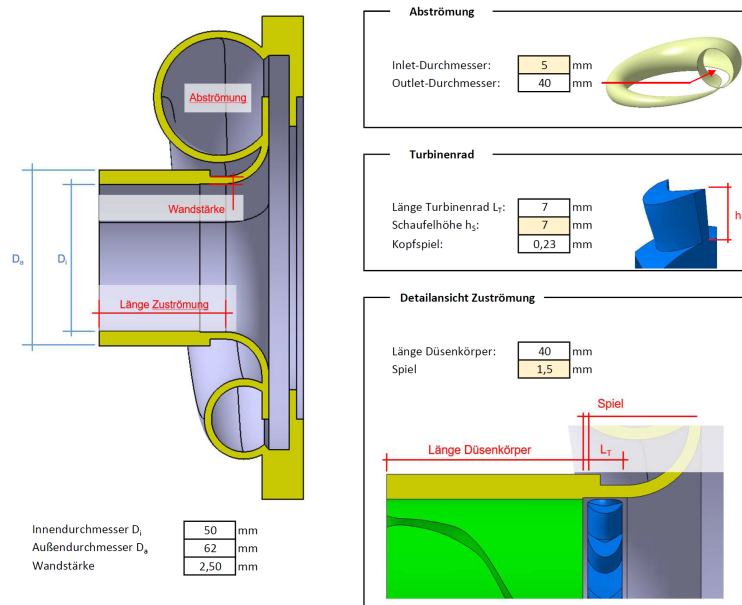


Figure 6 Results of the Microsoft Excel design tool with the spreadsheet for the shaft of the micro turbine

The aim is the automated parametric design of an Organic Rankine Cycle (ORC) turbine. This is to be realized using a macro with a graphical user interface. In the following, all steps that were necessary to create the macro will be explained. CATIA is a Computer Aided Design (CAD) Tool, which is taught at *htw saar* in the field of design. In Fig. 6 is a typical working screen with a turbine component [9]. The generated user interface consists of several tabs for the individual parts to be generated ("MultiPage" function), a background image and various input fields for the parameter values to be entered. Input fields are always in one layer in front of the background image, so their visibility is guaranteed. Logical names have also been assigned to the individual input fields, which are also marked with the parameter names.

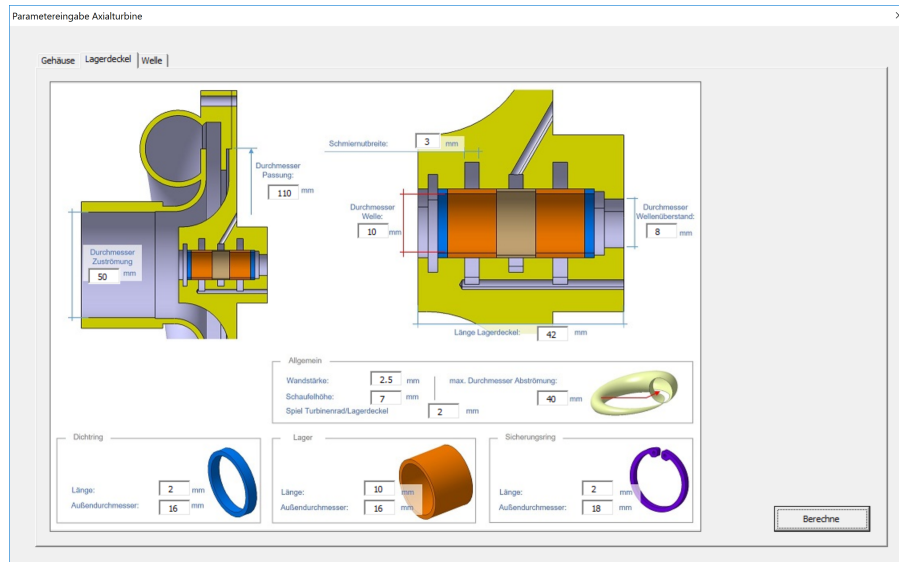


Figure 7 Screenshot of the graphical user interface of the design tool for the turbine model

4. Additive manufacturing

Additive manufacturing (AM) becomes more and more important because of a growing amount of available FDM printers on the market. In the laboratory of wind energy technologies are *Ultimaker 2* and *Ultimaker 2+* printers available. They are used for producing airfoils for wind turbine prototypes or testing. To improve efficiency of a small wind turbine and validate designs a new workflow was developed. The geometry parameters are also transfers to a mesh generator to create a discretization of the domain. The different rotor blades can be simulated and should be compared to measurement results. Thanks to additive manufacturing technology, a full workflow was developed, so these profiles can be printed out and mounted on a universal test rig.

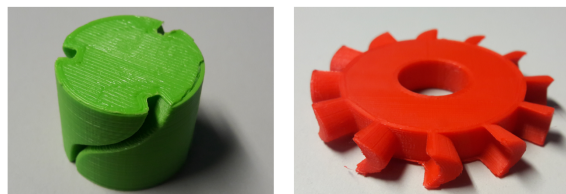


Figure 8 Additive manufactured Laval nozzle part (*left side*) and turbine rotor (*right side*) for the *Organic Rankine Cycle* (ORC) turbine for construction tests

Based on the CFD results, two values are calculated and passed over to the validation module. These are the average thrusts, which means the tangential force components in the direction of rotation that generates the power and its standard deviation within the considered space of flow variables. The maximization of the former and the minimization of the latter are the objective functions efficient and stable operation under varying wind conditions. Parallel to the simulation process the geometry will be generated (*Format: *.stl*) and is printed on the FDM printer.

5. Conclusions and outlook

In this paper the geometry of an Organic Rankine Cycle (ORC) turbine was constructed on the basis of computational fluid dynamics (CFD) calculations. This allows parameterized generation based on variable boundary conditions. After the components housing, bearing cap and shaft have been generated by the macro, the assembled turbine is shown here.

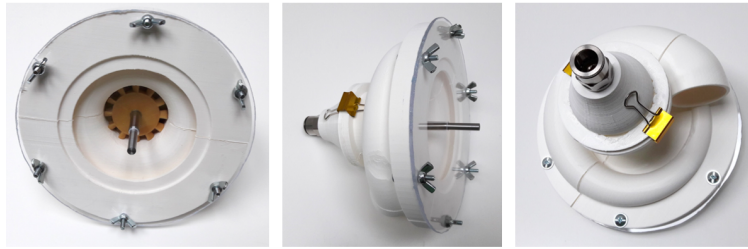


Figure 9 Additive manufactured prototype of the full Organic Rankine Cycle (ORC) turbine housing (scale 1:1)

The parameterization allows further improvements, especially with regard to the compensation of the axial forces occurring during operation. Axial forces that could remain uncompensated would cause the shaft to run against the bearing cap and damage it in the long term. These axial forces are only weak due to the chosen equal pressure blading, but it could nevertheless make sense to provide such an axial force compensation. This could be done hydraulically, for example.

In the presented turbine, a turbine wheel with 12 blades and a nozzle body with three nozzle channels evenly distributed over the circumference were used. Since the number of blades is an integral multiple of the number of nozzle channels, the nozzle outlet always has the same geometry as an impeller blade. This can lead to start-up difficulties. Accordingly, it could be cheaper not to distribute the three nozzle channels evenly over the circumference or to choose a higher number of blades of e.g. 16. The great advantage of this design is that the number of Laval nozzles in the nozzle part can be varied and the mass flow can therefore be adapted. Odd blade counts are rather unusual when designing turbines. In this case, however, changes to the number of blades are ruled out due to the size of the turbine wheel.

Since the turbine is to be used for energy recovery, a generator can be mounted directly on the same shaft as the turbine, but also a gearbox can be connected to reduce the extremely high speed to a suitable level (e.g. 20:1) which helps to protect the generator material.

Finally it can be said, that we presented our software tool that should help to generate a simple axial micro turbine for a defined mass flow of propane. But further investigations due to advanced construction aspects has to be done.

References

- [1] **Paulus, M.:** Wärmerückgewinnungspotenziale durch die Nutzung von Abgas an Walzwerk-öfen, *Bachelorarbeit, htw saar*, **2015**.
- [2] **Freymann, R., Strobl, W.:** Der Turbosteamer: Ein System zur Kraft-Wärme-Kopplung im Automobil, *MTZ*, 69, **2008**.
- [3] **Quoilin, S.:** Experimental Study and Modeling of a Low Temperature Rankine Cycle for Small Scale Cogeneration, PhD Thesis, *University of Liege*, **2007**.
- [4] **Ibaraki, S., Endo, T., Kojima, Y., Takahashi, K., Baba, T., Kawajiri, S.:** Study of Efficient On-board Waste Heat Recovery System Using Rankine Cycle, *Review of Automotive Engineering*, 28, 307–313, **2007**.
- [5] **Bredel, E., Nickl, J.:** Abwärmenutzung im Antrieb von Heute und Morgen, *MTZ*, 04, 72, **2001**.
- [6] **Ringler, J., Seifert, M., Guyotot, V., Hübner, W.:** Rankine Cycle for Waste Heat Recovery of IC Engines; SAE International; 2009-01-0174, **2009**.
- [7] **Perić, M., Ferziger, J. H.:** Computational Methods for Fluid Dynamics, *Springer*, **2002**.
- [8] Engineering Simulations and 3-D Design Software, Available online: www.ANSYS.com.
- [9] <https://www.3ds.com/de/produkte-und-services/catia>.
- [10] <https://www.plm.automation.siemens.com/de/products/lms/imagine-lab>.
- [11] **Noll, B.:** Numerische Strömungsmechanik, Berlin **1993**.
- [12] **Menter, F., Esch, T., Kubacki, S.:** Transition modelling based on local Variables, In Proceedings of the Fifth International Symposium on Engineering Turbulence Modelling and Measurements, Mallorca, Spain, 16–18 September 2002, Engineering Turbulence Modelling and Experiments 5. Rodi, W., Fueye, N., Eds., *Elsevier: Amsterdam, Netherlands*, 555–564, **2002**.
- [13] **Resch, M., Curre-Linde, N., Küster, U., Risio, B.:** A Grid Framework for Computational Mechanics Applications, Mastorakis, N. (Eds.), Proceedings of the *2nd WSEAS International Conference on Applied and Theoretical Mechanics (MECHANICS'06)*, 360–369, Venice, Italy, **2006**.
- [14] **Rückert, F. U., Ströhle, J., Sabel, T., Schnell, U., Hein, K. R. G.:** Advantages of Combining Different Grid Types for 3D Furnace Modelling, *Sixth International Conference on Technologies and Combustion for a Clean Environment*, Porto, Portugal, **2001**.
- [15] **Benim, A. C., Chattopadhyay, H., Nahavandi, A.:** Computational Analysis of turbulent forced Convection in a Channel with a triangular Prism, *Int. J. Therm. Sci.*, 50, 1973–1983, **2011**.
- [16] **Wursthorn, S.:** Numerische Untersuchung kavitierender Strömungen in einer Modellkreiselpumpe, *Universität Karlsruhe, Dissertation*, Karlsruhe, **2001**.

- [17] **Benim, A. C., Nahavandi, A., Syed, K.:** URANS and LES analysis of turbulent swirling flows, Progress in *Computational Fluid Dynamics An Int. J.*, 5, 444–454., **2005**.
- [18] **Barth, T. J., Jespersen, D.:** The Design and Application of upwind Schemes on unstructured Meshes, In Proceedings of the AIAA 27th Aerospace Sciences Meeting, Reno, NV, USA, *Technical Report*, AIAA-89-0366, **1989**.
- [19] **Durbin, P. A., Pettersson Reif, B. A.:** Statistical Theory and Modeling for Turbulent Flows, 2nd ed., *Wiley: Chichester*, UK, **2011**.
- [20] Roloff/Matek: Maschinenelemente, 21. Auflage, *Springer Vieweg*, **2013**.
- [21] Roloff/Matek: Maschinenelemente - Tabellenbuch, 21. Auflage, *Springer Vieweg*, **2013**.